Transactions, SMiRT-26
Berlin/Potsdam, Germany, July 10-15, 2022
Division II

Influence of PWR fuel assembly bow on RCCA drop

Jens Arndt[1], Christoph Bläsius[2], Jürgen Sievers[3]

[1] Expert Structure Mechanics (Jens.Arndt@grs.de) [2] Expert Structure Mechanics
[3] Chief Expert Structure Mechanics
Gesellschaft für Anlagen- und Reaktorsicherheit (GRS) gGmbH, Cologne, Germany

ABSTRACT

Fuel assembly bow in PWRs is a known issue for more than 20 years [1]. Extreme fuel assembly bow can cause considerably higher drop times of rod cluster control assemblies (RCCA) or even incomplete rod insertion events (IRI). In the paper the effects of fuel assembly bow on drop success, time and velocity are analyzed using a numerical Finite Element (FE)-model. For the simulation of the fluidic damping, the model employs an iterative fitting to experimental measurements. The results of the simulations reveal that the form of the bow, the grade of deflection and the friction coefficient have a significant influence on drop time. A strong non-linear increase of drop times can be observed for extreme deflections at higher deformation modes. The results are compared with simulated and measured data from literature.

INTRODUCTION

PWRs employ rod cluster control assemblies (RCCA) to control the neutronic activity in the core and force the reactor to a subcritical state as part of the safety system [2].
Fuel assembly bow in PWRs is a known issue for more than 20 years [1]. Extreme fuel assembly bow can cause considerably higher drop times or even incomplete rod insertion events (IRI). The identification of the main factors of influence and the quantification of safety margins require best-estimate analyses. Therefore, in the paper the influence of fuel assembly bow on drop success, time and velocity is assessed by a numerical model. For the simulation of the fluidic damping, the model employs an iterative fitting to experimental measurements. The analysis of RCCA drop kinetics was in the past subject of research by the German Reactor Safety Commission (RSK) [3], French Atomic Energy Commission (CEA) [7] and other relevant research projects [1] [4] [5] [6].

MODEL

A generic control rod (Fig. 1) consists of an austenitic steel tube with a jacket structure made of zircon alloy.

Fig. 1 Geometry and dimensions of the generic control rod [2]

Fig. 2 shows the geometry of the generic guiding tube which employs zircon alloy as base material [2]. The damper area is not yet considered. Interactions between different control rods in the same cluster with possibly different bow expression are not considered in the model as well.

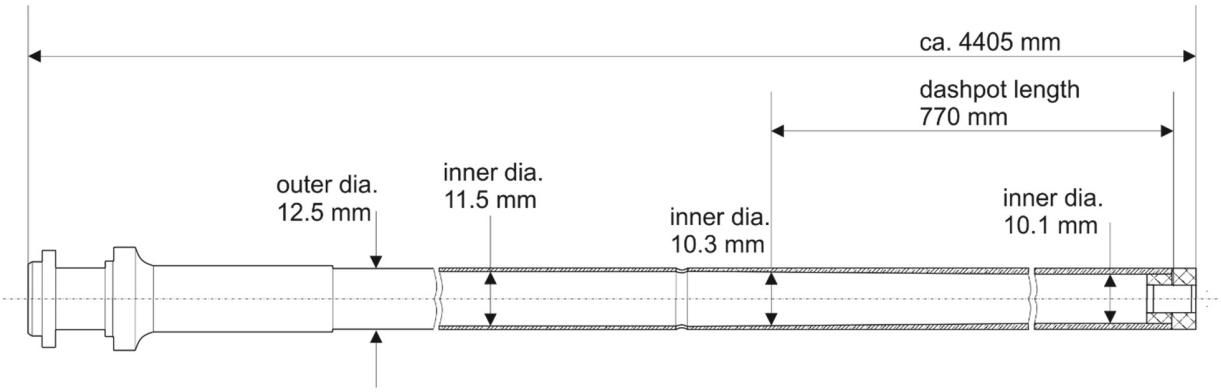

Fig. 2 Geometry and dimensions of the generic guiding tube [2]

The FE-program LS-DYNA [9] is employed for all simulations. The explicit solver is used for simulation of the drop process while the implicit solver is used for the calculation of the initial bow distribution. Fig. 3 displays a magnified view of the area where the control rod immerges into the guiding tube (shell element displayed with thickness).

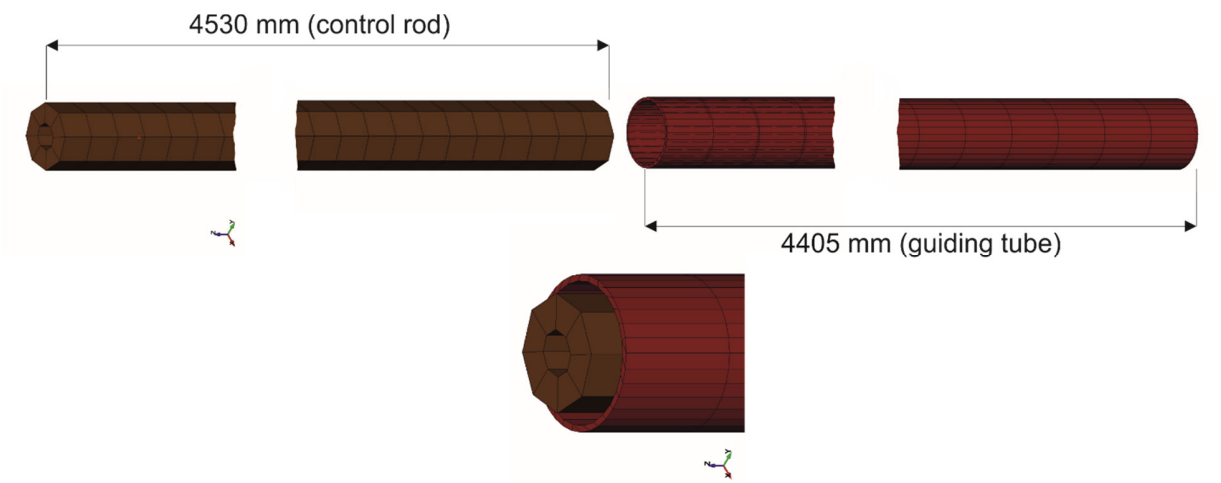

Fig. 3 FE-model of control rod and guiding tube

While the control rod is modelled by shell elements, the guiding tube is modelled by volume elements for practical reasons. Gravity acceleration of 9.81 m/s² is applied. Due to a fixed guiding tube, gravity only affects the control rod. For the friction coefficient of the surfaces a value of 0.30 is employed [12]. The recommended contact algorithm "*CONTACT_AUTOMATIC_SURFACE_TO_SURFACE" by LS-DYNA [9] is used. The algorithm is well-suited to handle disjoint meshes. In case of shell elements, it creates a contact surface in an adjustable distance to the shell. At the exterior edge, the contact surface wraps around the shell edge forming a continuous contact surface [9]. Due to the straight upper part of the guiding tube which block lateral and rotary displacements of the falling control rod the simulation was

accomplished without additional boundary conditions on the control rod model. The expected stresses are considerably below yield strength. Therefore, an elastic material law is employed. The guiding tube and the jacket of the control rod are made of zircon alloy, the inner tube inside the control rod is made of the austenitic steel (Tab. 1). For simplification purposes a fictive, homogenous material model of the whole control rod is considered which merges the values of the inner tube with the jacket. Furthermore, an additional mass of 0.145 kg is considered in the modified density value to account for the proportion of the auxiliary parts of the RCCA (Tab. 1).

Tab. 1 Material data [10] [12]

Material	Young's modulus [MPa]	Poisson's ratio	Density [kg/m³]
Zircon alloy	76000	0.3	6550
Austenitic steel	179000	0.3	7850
Fictive control rod material	156042	0.3	9318

The FE-Code LS-DYNA allows the definition of mass weighted damping by part ID for all motions including rigid body motions. The keyword command "*DAMPING_PART_MASS" is applied for damping definition F_D (Equation 1):

$$F_D = D_S * m * v \tag{1}$$

Hereby D_S defines the damping constant, m the mass and v the velocity. Because no data of the damping coefficient are available and a direct model of the fluid is complex, a damping coefficient is generated by fitting on experimental data from literature [8]. Therefore, experiments without any bow are iteratively recalculated until the velocity curves met (Fig. 4). The drop time is increased from 0.8 s to 1.76 s with damping. A damping coefficient of D_{sm} = 3.09 1/s is found and employed for all subsequent calculations.

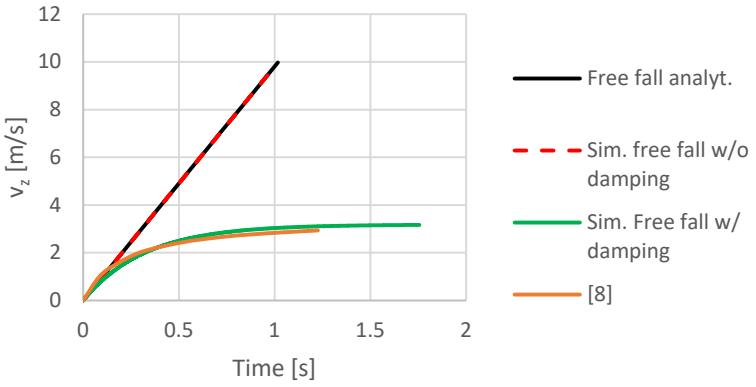

Fig. 4 Time-variant progress of velocity

For the validation of the undeformed model, the drop time of the undamped free fall without bow of 0.96 s is compared to the analytically calculated drop time t_e (Equation 2):

$$t_e = \sqrt{\frac{2*z}{g}} = \sqrt{\frac{2*4550mm}{9810\ mm/s^2}} = 0.963s \tag{2}$$

Three different bow modes (C-, S and W) are generated by implicit FE-simulation. The deformations are placed on a two-dimensional surface. Due to geometric restrictions of the fuel assembly (FA) the summation of displacements in the real reactor situation cannot exceed a maximum value of around 26 mm [3] (summation of gaps between FA and edge gap), which is taken here to determine the simulated deformation. C-bow is generated by a central (z=2202.5 mm) displacement in x-direction (Fig. 5).

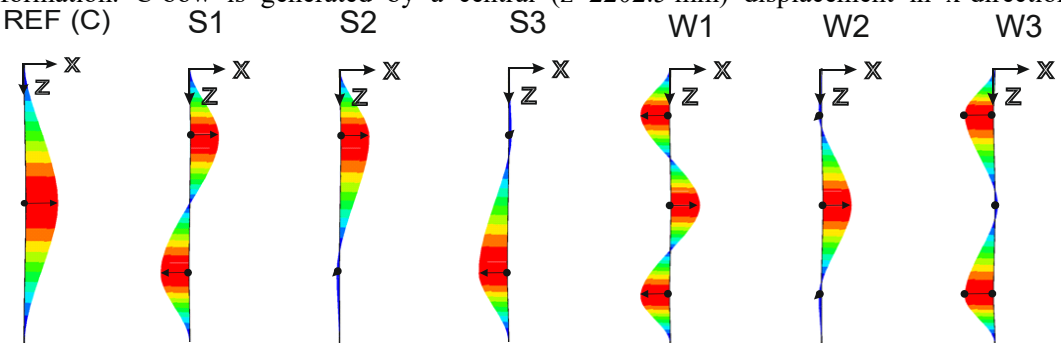

Fig. 5 C-bow, S-bow and W-bow modes of guiding tube

S-bow is generated by two defined displacements in x-direction, applied on z-coordinates z_1=1101.25 mm und z_2=3303.7 mm. Three different cases of S-bow are considered (Fig. 6):

- S1 (x_1=13 mm and x_2=-13 mm)
- S2 (x_1=24 mm and x_2=-2 mm)
- S3 (x_1=2 mm and x_2=-24 mm)

W-bow is generated by three displacements in x-direction. The displacements are applied on z-coordinates z_1=734.67 mm, z_2=2202.5 mm und z_3=3670.83 mm. Three different cases of W-bow are considered (Fig. 6):

- W1 (x_1=-13 mm, x_2=13 mm, and x_3=-13 mm)
- W2 (x_1=-2 mm, x_2=24 mm, and x_3=-2 mm)
- W3 (x_1=-24 mm, x_2=2 mm, and x_3=-24 mm)

RESULTS

In Tab. 2 drop times of different C-bow geometries and the time increase compared to the simulation without deformation are compared. A deformation of 26 mm from side to side causes an increase of drop time by 0.04 s compared to the undeformed geometry. Only assumed deformations which exceed the geometrical limit would cause a significant higher increase of drop times.

Table 2: Drop times of C-bow geometries with different bow grades

Run#	Bow geometry	Friction coefficient	Drop time
REF	None	0.3	1.75 s
C2	C (20 mm)	0.3	1.78 s (+0.03 s)
C3	C (26 mm)	0.3	1.79 s (+0.04 s)
C4	C (50 mm)	0.3	1.9 s (+0.15 s)
C5	C (70 mm)	0.3	2.07 s (+0.32 s)
C6	C (100 mm)	0.3	3.11 s (+0.36 s)

In Fig. 6 the time dependence of the vertical velocity is displayed. Deflected geometries show a significant horizontal oscillation at the lower end of the control rod. Probably the employed contact algorithm together with the fluidic damping also working in horizontal direction excites the oscillation. The development of the vertical travel is shown in Fig. 7. From a drop travel of ca. 2.5 m on, a high loss of velocity due to the onset of three-point-bending can be observed.

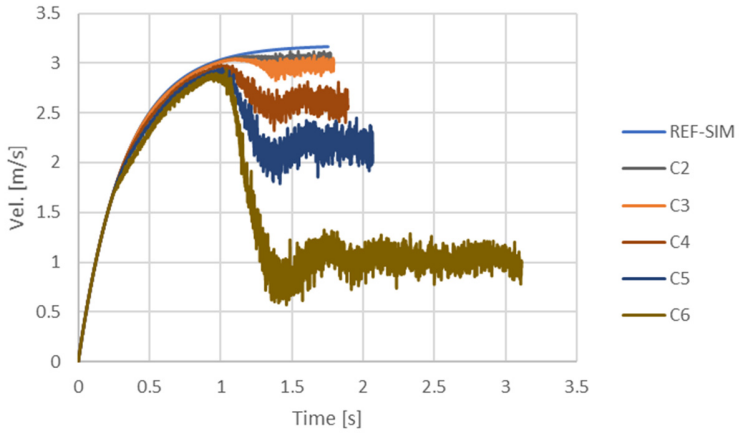

Fig. 6 Vertical velocity (influence of deformation grade, C-bow)

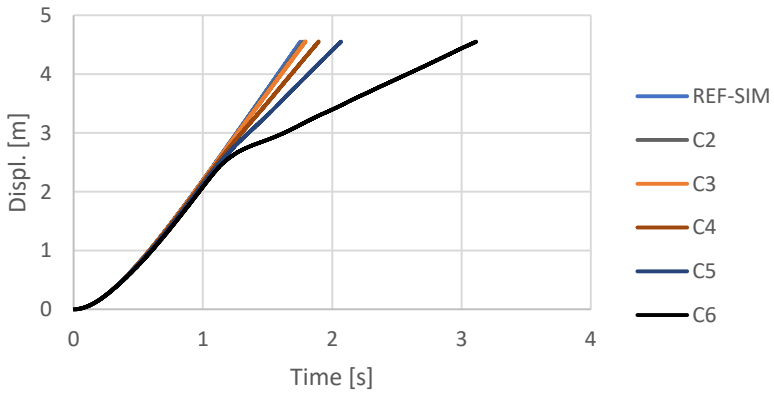

Fig. 7 Vertical displacement (influence of deformation grade, C-bow)

In Tab. 3 the drop times of deformed geometries with C-bow and a deflection of 26 mm for different friction coefficients are compared. The friction coefficient in the investigated range has a linear influence on the increase of the drop times as expected.

Table 3: Drop times of C-bow geometries with different friction coefficients

Run#	Bow geometry	Friction coefficient	Drop time
R1	C (26 mm)	0.3	1.79 s
R2	C (26 mm)	0.5	1.82 s (+0.03 s)
R3	C (26 mm)	0.7	1.85 s (+0.06 s)
R4	C (26 mm)	1.0	1.90 s (+0.11 s)

In Tab. 4 drop times of guiding tubes with C-, S- and W-bow are compared. For all bows a total deformation of 26 mm from side to side is assumed. The C-bow shows the lowest influence on the drop time compared to the reference without deformation. As expected, the S-bow with a high deformation (S2) has a significant influence on drop time (0.23 s higher compared to the undeformed guide tube).

Table 4: Drop times of different bow geometries

Run#	Bow geometry	Friction coefficient	Drop time
REF	None	0.3	1.75 s
C3	C (26 mm)	0.3	1.79 s (+0.04 s)
S1	S (13 mm/-13 mm)	0.3	1.83 s (+0.08 s)
S2	S (24 mm/-2 mm)	0.3	1.98 s (+0.23 s)
S3	S (2 mm/-24 mm)	0.3	1.80 s (+0.05 s)
W1	W (-13 mm/13 mm/-13 mm)	0.3	2.16 s (+0.41 s)
W2	W (-2 mm/24 mm/-2 mm)	0.3	1.92 s (+0.17 s)
W3	W (-24 mm/2 mm/-24 mm)	0.3	3.4 s (+1.65 s)

The W-bow with a high deformation in the upper and lower area (W3) shows an even higher influence on the drop time (1.65 s higher drop time compared to undeformed guide tube). For configuration W3, the rod is even stopped 80 mm before reaching the bottom of the model. In Fig. 8 and Fig. 9 the development of the vertical velocity and the vertical displacement are displayed.

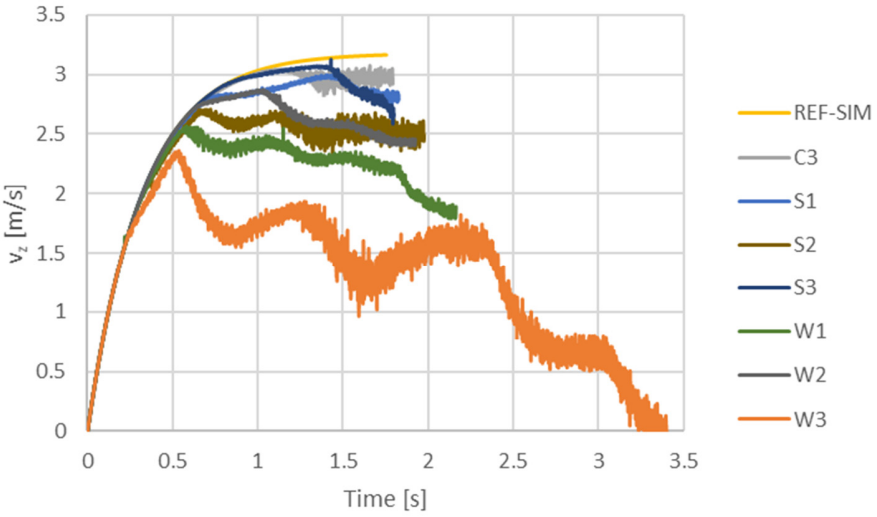

Fig. 8 Vertical velocity (influence of bow mode)

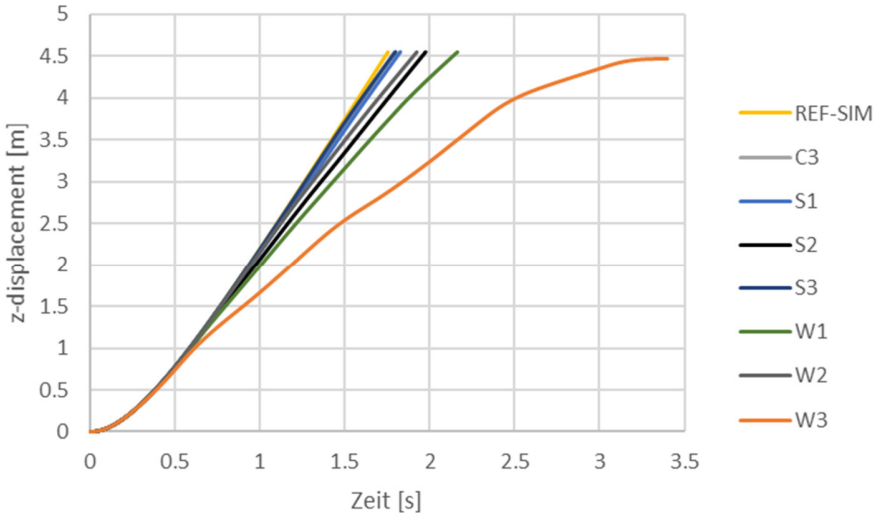

Fig. 9 Vertical displacement (influence of bow mode)

COMPARISON TO LITERATURE

The comparison to literature data [4] for the control rod drop with fuel assembly bow allows an assessment of the simulation results (Tab. 5). In this context it should be mentioned that unlike in [4], the damper, which is located at the lower stopper of the guiding tube, was not simulated. A simulation with consideration of the control rod drop with damper would probably cause significantly higher drop times. The simulated drop times for the straight geometry (C 0 mm) are identical (1.75 s). The drop time from [4] for a 30 mm C-bow is higher than the calculated times for a C-bow of 26 mm (0.21 s). Also, the related drop time of the S-bow (15 mm/-12 mm) [4] differs by 0.17 s from the time of the considered S-bow (13 mm/-13 mm).

Tab. 5 Comparison with drop times from literature

Run#	Bow geometry	Drop time
REF	None	1.75 s
C3	C (26 mm)	1.79 s (+0.04 s)
C4	C (50 mm)	1.90 s (+0.15 s)
C5	C (70 mm)	2.07 s (+0.32 s)
[4]	C (0 mm)	1.75 s (sim.) (+0 s)/ 1.85 s (exp.) (+0.1 s)
[4]	C (30 mm)	2.0 s (sim.) (+0.25 s)/ 2.7 s (exp.) (+0.95 s)
S1	S (13 mm/-13 mm)	1.83 s (+0.08 s)
S2	W (24 mm/-2 mm)	1.98 s (+0.23 s)
S3	W (2 mm/-24 mm)	1.8 s (+0.05 s)
[4]	S (15 mm/-12 mm)	2.0 s (sim.) (+0.25 s) / 2.1 s (exp.) (+0.35 s)

The numerical model from Collard [8] is quite similar to the GRS model but due to a lack of geometrical details a comparison has not been made.

CONCLUSION

In the paper the effects of fuel assembly bow on drop success, time and velocity were analyzed by a numerical model. In the model different simplifications and approximations concerning material model, geometry, boundary conditions and application of forces were assumed. An important conclusion is the observation that the bow mode, the grade of deflection and the friction coefficient have a significant influence on the drop time of a control rod. A strong non-linear increase of drop times with increasing bow deflection can be observed. The influence of the cross-section geometry and stiffness of the guiding tube and control rod was not yet investigated. A very limited comparison with measured and calculated data [4] was done. Further development of the model may consider the following:

- Extended validation of the contact formulation as the crucial element of the model
- Enhanced consideration of boundary conditions, such as flexibility of the guide tube
- Addition of the damper part of the guiding tube to the existing model
- Simulation of water induced damping in the guiding tube by fluid elements

Therefore, significant influence factors on the drop time have been identified but the calculated results still include some uncertainties which should be investigated in further detail.

ACKNOWLEDGEMENT

The work has been performed in the framework of the Reactor Safety Research Program of the German Federal Ministry for the Environment, Nature Conservation and Nuclear Safety and Consumer Protection (BMUV).

REFERENCES

[1] Aulló, M., Aleshin, A., Messier, J.: Reduction of Fuel Assembly Bow with the RFA Fuel, Paper, 2012
[2] U.S. NRC, U.S. EPR Application Documents, ML13220A677 - AREVA Design Control Document, Fuel System Design, 2013
[3] RSK-Report 474, Session of German Reactor Safety Commission (RSK): Deformation of fuel assembly in German PWR, http://www.rskonline.de/sites/default/files/reports/epanlagersk474hp.pdf
[4] Bosselut, D., Andriambololona, H.: Drop and drop of control rod in assembly, EDF R & D France, 2004
[5] Wanninger, A., Seidl M., Macián-Juan, R.: Mechanical analysis of the bow deformation of a row of fuel assemblies in a PWR core, Nuclear Engineering and Technology, Vol. 50, pp. 297-305, 2018
[6] Aleshin, Y.: Plant and Cycle Specific Fuel Assembly Bow Evolution Assessment, 2017 Water Reactor Fuel Performance Meeting, Jeju Island, Korea, 2017
[7] Lascar, C., Champigny, J., Chatelain, A., Chazot, B., Goreaud, N., Mery de Montigny, E., Pacull, J., Salaün, H.: Advanced Predictive Tool for Fuel Assembly Bow based on a 3d coupled FSI Approach, AREVA, 2015
[8] Collard, B.: Rod cluster control assembly drop kinetics with seismic excitation, 7th international conference on nuclear engineering, Tokyo, Japan, April 10-23, 1999
[9] LS-DYNA Keyword user's manual, LS-DYNA R11 (r:10580), Livermore Software Technology Corporation (LSTC), 2018
[10] U.S. NRC, BAW-10227-A - Evaluation of Advanced Cladding and Structural Material (M5) in PWR Reactor Fuel, 2000

[11] Sonnenburg, H.-G., Arndt, J., Bals, Ch., Herb, J., Sievers, J.: Methods for the analysis of fuel rod behavior under operating conditions and the conditions for loss of coolant (LOCA) and reactivity accidents (RIA), RS1193, GRS-A-3717, 2013

[12] Grote, K.-H., Feldhusen, J.: Dubbel, Handbook of mechanical engineering, Chapter B14, Mechanics of rigid bodies, Tab. 4: Friction coefficients, 22th Edition, 2007

[13] ThyssenKrupp Materials, Material data sheet, TK 1.4404, 2006